

High Pressure Synthesis of Marcasite-Type Rhodium Pernitride

Ken Niwa,^{*,†} Dmytro Dzivenko,[‡] Kentaro Suzuki,[†] Ralf Riedel,[‡] Ivan Troyan,[§] Mikhail Eremets,[§] and Masashi Hasegawa[†][†]Department of Crystalline Materials Science, Nagoya University, Furo-cho, Chikusa-ku, Nagoya 464-8603, Japan[‡]Fachgebiet Disperse Feststoffe, Fachbereich Material- und Geowissenschaften, Technische Universität Darmstadt, Jovanka-Bontschits-Str. 2, 64287 Darmstadt, Germany[§]Department of Biogeochemistry, Max-Planck-Institut für Chemie, Hahn-Meitner-Weg 1, 55128 Mainz, Germany

Supporting Information

ABSTRACT: Marcasite-type rhodium nitride was successfully synthesized in a direct chemical reaction between a rhodium metal and molecular nitrogen at 43.2 GPa using a laser-heated diamond-anvil cell. This material shows a low zero-pressure bulk modulus of $K_0 = 235(13)$ GPa, which is much lower than those of other platinum group nitrides. This finding is due to the weaker bonding interaction between metal atoms and quasi-molecular dinitrogen units in the marcasite-type structure, as proposed by theoretical studies.

Nitrides are attractive materials not only in the field of fundamental crystal chemistry but also in industrial applications.¹ In the 2000s, platinum group nitrides (PtN_2 , OsN_2 , IrN_2 , and PdN_2) were remarkably discovered in a direct chemical reaction between platinum group elements and molecular fluid nitrogen at high pressures and temperatures.^{2–7}

The new class of compounds attracted much attention due to the unusual crystal chemistry as well as intriguing mechanical properties (e.g., $K_0 = 428$ GPa for IrN_2) owing to the strong bonding interaction between noble metals and nitrogen.^{2–7} However, to the best of our knowledge, there has been no experimental evidence of a successful synthesis of rhodium nitride so far, although theoretical studies suggest that rhodium is likely to form RhN_2 with a marcasite-type structure.^{8,9}

We now succeeded in the synthesis of marcasite-type rhodium nitride in a direct chemical reaction between rhodium metal and molecular nitrogen at 43.2 GPa in a laser-heated diamond-anvil cell (LH-DAC). The results are in good agreement with the theoretical prediction.^{8,9} We report here the details of the synthesis experiments including characterization of the product via high pressure in situ Raman and X-ray diffraction (XRD) measurements and scanning electron microscopy (SEM) combined with energy dispersive X-ray (EDX) analysis after recovering the sample at ambient conditions.

Figure 1(a) shows the XRD pattern of the sample that was measured after heating at 43.2 GPa. The details of the experimental setup are described in the Supporting Information. Several sharp reflections (labeled with miller indices hkl) were found, in addition to the diffraction peaks that correspond to the residual rhodium metal¹⁰ and solid nitrogen.¹¹ The new reflections were perfectly indexed for an orthorhombic cell with

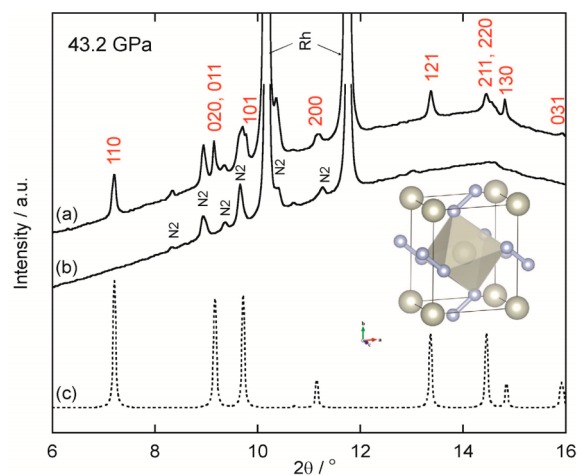


Figure 1. (a) XRD pattern of the sample measured after heating at 43.2 GPa. The diffraction peaks, which are labeled with the Miller indices, correspond to marcasite-type rhodium nitride, RhN_2 . Other peaks are due to the residual rhodium metal¹⁰ and solid nitrogen.¹¹ (b) XRD pattern of the unheated region. N_2 represents the solid nitrogen with a rhombohedral structure.¹¹ (c) Simulated XRD pattern of marcasite-type RhN_2 at 43.2 GPa together with a schematic illustration of the crystal structure for marcasite-type RhN_2 . Large and small balls represent rhodium and nitrogen atoms, respectively. The lattice constants and atomic positional parameters were taken from the present results and from the theoretical calculation study,⁸ respectively.

the lattice parameters of $a = 3.847(5)$ Å, $b = 4.683(5)$ Å, and $c = 2.696(6)$ Å (at 43.2 GPa), which is consistent with earlier predicted marcasite-type structures (space group $Pnmm$).^{8,9}

Therefore, it can be concluded unambiguously that rhodium reacted with nitrogen to form marcasite-type RhN_2 above 43 GPa. The presence of the new reflections was clearly identified during the decompression process to the pressure of approximately 10 GPa, while immediately after the release of the pressure the reflections broadened significantly (Figures S1 and S2, Supporting Information). Although the diffraction lines of the recovered marcasite-type RhN_2 were rather broad with less intensity, they could be resolved, and the lattice constants could be calculated (Figure S2, Supporting Information). Accordingly, the lattice parameters of marcasite-type RhN_2 at

Received: November 20, 2013

Published: January 6, 2014

ambient pressure were analyzed to be $a_0 = 3.982(1) \text{ \AA}$, $b_0 = 4.858(1) \text{ \AA}$, and $c_0 = 2.834(1) \text{ \AA}$, which are close to the results of the theoretical calculations.^{8,9} The obtained lattice parameters and volume of the unit cell of marcasite-type RhN_2 are listed in detail in Table S1 of the Supporting Information, together with those of the theoretical studies. The fine grains of less than 100 nm in size were identified by SEM on the sample surface close to the heated regions (Figure S3, Supporting Information); however, the chemical composition could not be determined mainly due to the fundamental instability of marcasite-type RhN_2 as identified from the broadness of diffraction peaks or large amount of residual rhodium metal.

Vibration spectroscopy analysis, combined with theoretical calculations, offers useful information on the electronic valence state and the bonding nature of nitrogen in the metal nitrides.^{5,6,13} Figure 2 represents the Raman spectrum of the

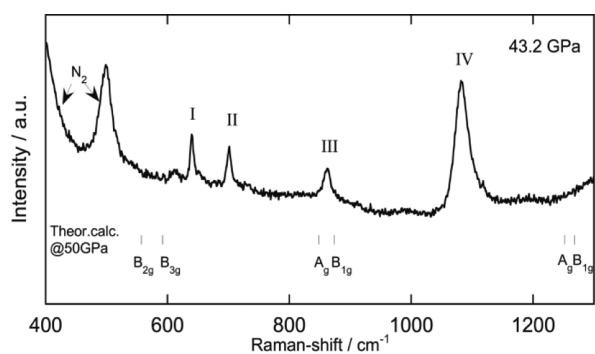


Figure 2. Raman spectrum of the sample after being heated at 43.2 GPa, together with the theoretical prediction at 50 GPa.⁸ Peaks labeled I, II, III, and IV correspond to marcasite-type RhN_2 . Intense peaks at the low-frequency region stem from solid nitrogen.¹²

sample that was measured after heating at 43.2 GPa. The Raman spectrum did not change even after heating for long time at 43.2 GPa. We found at least three sharp and one broad bands (denoted as I, II, III, and IV in Figure 2), and no other peaks were detected in the wavenumber region of the present study. Taking into account the results of the high pressure in situ XRD measurement, it is concluded that the Raman spectrum corresponds to marcasite-type RhN_2 . The group theory analysis gives six active Raman modes ($\Gamma = 2A_g + 2B_{1g} + B_{2g} + B_{3g}$) for marcasite-type TX_2 , and the Raman frequency modes are assigned with respect to the dumbbell-like X–X units.¹⁴ The vibron frequency of dinitrogen in pernitrides or molecules strongly depends on the bonding character, such as N–N ($\sim 1.4 \text{ \AA}$, $\sim 800 \text{ cm}^{-1}$),¹⁵ N=N ($1.2\text{--}1.3 \text{ \AA}$, $1300\text{--}1550 \text{ cm}^{-1}$),^{16–21} and N≡N ($\sim 1.1 \text{ \AA}$, $\sim 2400 \text{ cm}^{-1}$).^{11,15} Spectroscopic approaches combined with theoretical calculations have also been applied to platinum group metal nitrides.^{5,6,13} Recent theoretical calculation studies reported that Pt^{4+} and N_2^{4-} are the correct electronic valence states for PtN_2 .¹³ The anion N_2^{4-} is isoelectronic with that of the fluorine molecule, and the N–N bond length is well consistent with the F–F bond length (1.42 \AA).¹³ Furthermore, the strong Raman peak ($\sim 800 \text{ cm}^{-1}$) for PtN_2 is well consistent with that of single-bonded polymeric nitrogen.^{5,13,15} These findings strongly suggested that dinitrogen (N–N) in PtN_2 exhibits a single-bond nature. In the case of rhodium pernitride, the Raman peak frequency ($\sim 1100 \text{ cm}^{-1}$) characterized as dinitrogen is higher than that of PtN_2 ^{5,13} and single-bonded polymeric nitrogen ($\sim 800 \text{ cm}^{-1}$),¹⁵ while it

is lower than the frequency of $1300\text{--}1550 \text{ cm}^{-1}$, which corresponds to double-bonded nitrogen deduced from N_2H_2 and alkaline earth diazenides.^{13,20,21} This observation indicates that the bond length of dinitrogen in marcasite-type RhN_2 is intermediate between single- and double-bonded dinitrogen. Further detailed discussion with respect to the Raman scattering measurements are described in Figures S4 and S5 of the Supporting Information.

The elastic properties of marcasite-type RhN_2 are evaluated based on the high pressure in situ XRD measurements. As shown in Figure 3(a), the a - and b -axes of marcasite-type RhN_2

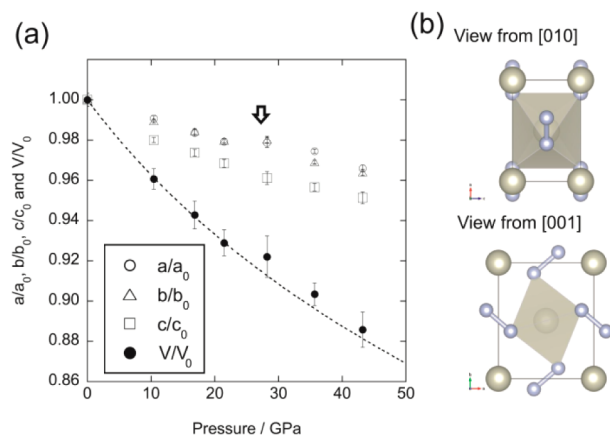


Figure 3. (a) Normalized lattice parameters and volume of marcasite-type RhN_2 as a function of pressure. Dashed line represents a result of the B–M EOS fitting to the present data below 21 GPa because of the discontinuity around 25 GPa as indicated by the open arrow. The EOS is extrapolated to higher pressure with $K_0 = 235(13) \text{ GPa}$ and $K'_0 = 5.9(1.8)$. (b) Schematic illustrations of the crystal structure of marcasite-type RhN_2 viewed from $[010]$ and $[001]$ directions. Large and small balls represent rhodium and nitrogen atoms, respectively. Rhodium atoms are coordinated by six nitrogen atoms, and each RhN_6 octahedra are connected by N–N units.

show similar compressibility between each other, while the c -axis is more compressed than the other two-axes. The order of axial compressibility is consistent with the result of the recent high pressure experiment on marcasite-type FeP_2 .²² From the schematic illustration of the crystal structure viewed from different axes (Figure 3(c)), it is reasonable to assume the rotation of the RhN_6 octahedron in the a – b plane and the distortion along the c -axis to be the dominant compression mechanism. The alignment of N–N also plays an important role for the anisotropic axial compressibility of marcasite-type RhN_2 . The DFT calculation suggested that bonding interactions between nitrogen and the noble metal atom (Ru and Rh) are weak, and the N–N distance in these two nitrides are shorter than that of other noble metal nitrides (PtN_2 , OsN_2 , and IrN_2).⁸ The neighboring RhN_6 octahedra are connected via bonded N–N. This also plays a role to block the rotation of the RhN_6 octahedra with the pressure, which finally results in a lower compressibility of the a - and b -axes. In contrast, the most compressed c -axis indicates that the RhN_6 octahedra were largely distorted along their equatorial direction, and the N–N seemed not to affect the compressibility along the c -axis. The pressure–volume data below 21 GPa were fitted to the Birch–Murnaghan equation of state because the discontinuity was found in the compression curve at about 25 GPa. This procedure yields a zero-pressure bulk modulus of $K_0 = 235(13)$

GPa ($K'_0 = 5.9(1.8)$). Although the present data were carefully and repeatedly analyzed, the discontinuity accompanying with the volume expansion at high pressure still remained. It seems difficult to accept this behavior based on the physical points of view, and many more data points would offer a much clear conclusion. On the other hand, a new Raman peak denoted as V (Figure S4, Supporting Information) appeared at a pressure of 28 GPa, which corresponds to the onset pressure where the discontinuity was detected in the pressure–volume data. This indicates that a change of the vibration property in the dinitrogen (N–N) might strongly correlate with the bulk compression mechanism of RhN_2 . The incorporation of molecular nitrogen into the lattice of RhN_2 under high pressure might also expand the unit cell volume. In order to clarify these, further detailed experimental and theoretical investigations would be required. The obtained bulk modulus is 100–200 GPa lower than those of PtN_2 , OsN_2 , and IrN_2 as reported in previous studies,^{2–4} and it is in reasonable agreement with the theoretical zero-pressure bulk modulus of $K_0 = 286$ GPa ($K'_0 = 5.58$)⁸ (Table S2, Supporting Information). The low zero-pressure bulk modulus of $K_0 = 235(13)$ GPa is due to the weak bonding interaction between metal atoms and quasi-molecular dinitrogen units in the marcasite-type structure, as proposed by theoretical studies.

■ ASSOCIATED CONTENT

● Supporting Information

Details of experimental setup and results of high pressure in situ XRD and Raman scattering measurements. This material is available free of charge via the Internet at <http://pubs.acs.org>.

■ AUTHOR INFORMATION

Corresponding Author

*E-mail: niwa@numse.nagoya-u.ac.jp.

Author Contributions

All authors have given approval to the final version of the manuscript.

Notes

The authors declare no competing financial interest.

■ ACKNOWLEDGMENTS

We are thankful for the technical support of Drs. S. Besedin, H. Wang, and P. Naumov for performing the Raman measurements and gas loading. We are also thankful for the support of Dr. M. Mezouar for the synchrotron experiment. This research was supported by the Young Researcher Overseas Visits Program for Vitalizing Brain Circulation from the Ministry of Education, Culture, Sports, Science and Technology of Japan.

■ REFERENCES

- (1) (a) Oyama, S. T. In *The Chemistry of Transition Metal Carbides and Nitrides*; Blackie Academic & Professional, Chapman & Hall: Glasgow, 1996. (b) Ivanovskii, A. L. *Russ. Chem. Rev.* **2009**, *78*, 303.
- (2) Gregoryanz, E.; Sanloup, C.; Somayazulu, M.; Badro, J.; Fiquet, G.; Mao, H. K.; Hemley, R. J. *Nat. Mater.* **2004**, *3*, 294.
- (3) Young, A. F.; Sanloup, C.; Gregoryanz, E.; Scandolo, S.; Hemley, R. J.; Mao, H. K. *Phys. Rev. Lett.* **2006**, *96*, 155501.
- (4) Crowhurst, J. C.; Goncharov, A. F.; Sadigh, B.; Evans, C. L.; Morrall, P. G.; Ferreira, J. L.; Nelson, A. J. *Science* **2006**, *311*, 1275.
- (5) Young, A. F.; Montoya, J. A.; Sanloup, C.; Lazzeri, M.; Gregoryanz, E.; Scandolo, S. *Phys. Rev. B* **2006**, *73*, 153102.
- (6) Montoya, J. A.; Hernandez, A. D.; Sanloup, C.; Gregoryanz, E.; Scandolo, S. *Appl. Phys. Lett.* **2007**, *90*, 011909.

- (7) Crowhurst, J. C.; Goncharov, A. F.; Sadigh, B.; Zaug, J. M.; Aberg, D.; Meng, Y.; Prakapenka, V. B. *J. Mater. Res.* **2008**, *23*, 1.
- (8) Yu, R.; Zhan, Q.; De Jonghe, L. C. *Angew. Chem., Int. Ed.* **2007**, *46*, 1136.
- (9) Hernández, E. R.; Canadell, E. J. *Mater. Chem.* **2008**, *18*, 2090.
- (10) Perez-Albuern, E. A.; Forsgren, K. F.; Drickamer, H. G. *Rev. Sci. Instrum.* **1964**, *35*, 29.
- (11) Olijnyk, H. J. *Chem. Phys.* **1990**, *93*, 8968–8972.
- (12) Schneider, H.; Hiifner, W.; Wokaun, A.; Olijnyk, H. J. *Chem. Phys.* **1992**, *96*, 8046.
- (13) Wessel, M.; Dronskowski, R. *J. Am. Chem. Soc.* **2010**, *132*, 2421.
- (14) Lutz, H. D.; Müller, B. *Phys. Chem. Minerals* **1991**, *18*, 265.
- (15) Eremets, M. I.; Gavriluk, A. G.; Trojan, I. A.; Dzivenko, D. A.; Boehler, R. *Nat. Mater.* **2004**, *3*, 558.
- (16) Vajenine, G. V.; Auffermann, G.; Prots, Y.; Schnelle, W.; Kremer, R. K.; Simon, A.; Knier, R. *Inorg. Chem.* **2001**, *40*, 4866.
- (17) Auffermann, G.; Prots, Y.; Knier, R. *Angew. Chem., Int. Ed.* **2001**, *40*, 547.
- (18) Schneider, S. B.; Frankovsky, R.; Schnick, W. *Inorg. Chem.* **2012**, *51*, 2366.
- (19) Schneider, S. B.; Frankovsky, R.; Schnick, W. *Angew. Chem., Int. Ed.* **2012**, *51*, 1873.
- (20) Bondybey, V. E.; Nibler, J. W. *J. Chem. Phys.* **1973**, *58*, 2125.
- (21) Auffermann, G.; Prots, Y.; Knier, R.; Parker, S. F.; Bennington, S. M. *Chem. Phys. Chem.* **2002**, *9*, 815.
- (22) Wu, X.; Kanzaki, M.; Qjn, S.; Steinle-Neumann, G.; Dubrovinsky, L. *High Pressure Res.* **2009**, *29*, 235.